EFFECTS OF METABOLIC INHIBITION ON THE MEMBRANE PROPERTIES OF ISOLATED MOUSE PRIMARY SENSORY NEURONES

By MICHAEL R. DUCHEN

From the Department of Physiology, University College London, Gower Street, London WC1E 6BT

SUMMARY

1. The patch-clamp technique has been used to investigate the mechanisms that couple membrane excitability to metabolism in neurones isolated from mouse dorsal root ganglia.

2. Blockade of electron transport by cyanide (CN^-), reduction of the mitochondrial membrane potential with carbonyl cyanide *p*-trifluoromethoxyphenyl hydrazone (FCCP), removal of glucose or inhibition of glycolysis with iodoacetic acid (IAA), all increased a K^+ conductance (g_K), which could be sufficient to shunt action potentials.

3. The K^+ conductance was reduced by incubation of cells in Ca^{2+}-free solutions or by increasing the Ca^{2+} buffering power of pipette-filling solutions. The Ca^{2+} ionophore, ionomycin, also increased a K^+ conductance, and current fluctuation analysis showed that the channels carrying the current induced by both ionomycin and by CN^- had a similar mean conductance of *circa* 9 pS. Thus, increased g_K was a Ca^{2+}-dependent K^+ conductance, $g_{K(Ca)}$, reflecting a rise in resting $[Ca^{2+}]_i$.

4. The conductance was not affected by inclusion of ATP or an ATP-regenerating system in the pipette, suggesting that the underlying rise in $[Ca^{2+}]$ is not due directly to loss of ATP, and confirming that the increased g_K is not carried through ATP-dependent K^+ channels.

5. Voltage-gated K^+ currents evoked by membrane depolarization were increased by CN^- or glucose removal. The current–voltage relation of the increased g_K mirrored the voltage dependence of Ca^{2+} entry, and thus reflects impaired cellular handling of the Ca^{2+} load imposed by depolarization.

6. The rise in $[Ca^{2+}]_i$ and altered Ca^{2+} buffering capacity induced by metabolic blockade affected several other conductances: (i) a Ca^{2+}-dependent chloride current was increased. (ii) Both the low-threshold transient and high-threshold sustained voltage-gated Ca^{2+} currents were attenuated and their thresholds were shifted in the hyperpolarizing direction. (iii) The inward current activated by hyperpolarization, I_H, seen in large cells, was attenuated by either metabolic blockade or ionomycin.

7. The responses of these neurones to impaired metabolism thus depend largely on the effects of raised $[Ca^{2+}]_i$ on the populations of channels expressed by the cells. These changes in membrane properties could account for some of the changes in neuronal behaviour seen during the clinical states of hypoxia or hypoglycaemia, underlying changes in central nervous system function.

13-2

INTRODUCTION

The objective of the present study was to define the cellular events that couple alterations in cell metabolism to altered membrane function in mammalian neurones. Reduced availability of oxygen or oxidizable substrate lead rapidly to profound changes in the function of the central nervous system. These changes are initially reversible, and no permanent neurological deficit is expected following syncope from vaso-vagal episodes or from transient hypoglycaemic episodes, as long as the duration of the insult is limited. Under such conditions, the EEG becomes silent (Grossman & Williams, 1971; Hansen, 1985). Electrophysiological studies in both whole animals or in hippocampal slices *in vitro* have shown that hippocampal, cortical and spinal neurones hyperpolarize and synaptic transmission fails (Eccles, Loyning & Oshima, 1966; Glötzner, 1967; Godfraind, Kawamura, Krnjević & Pumain, 1971; Krnjević, 1975; Lipton & Whittingham, 1979; Cox & Bachelard, 1982; Fujiwara, Higashi, Shimoji & Yoshimura, 1987; Krnjević & Leblond, 1987). Later, extracellular potassium rises (Van Harreveld, 1959; Branston, Strong & Symon, 1977; Hansen, Hounsgaard & Jahnsen, 1982; Hansen, 1985). The cellular mechanisms underlying the hyperpolarization remain uncertain. It has been assumed by several of the above authors that the hyperpolarization results from an increased calcium-activated potassium conductance $g_{K(Ca)}$, but evidence has remained equivocal (e.g. see Fujiwara *et al.* 1987).

In studies of whole animals, changes in metabolism initiate changes in the concentrations of ions, metabolites and transmitters in the extracellular space, in blood pressure and perfusion, and hormonal changes in response to the stress. The architectural and functional complexity of neural tissue has made it difficult to identify the basic pathophysiological changes in single neurones, even in studies of CNS slices. In the present study, the whole-cell patch-clamp technique has been used to study the electrophysiological responses of isolated single cells to alterations in metabolism. The technique allows complete control of the extracellular environment, and gives access to the intracellular space, while allowing the study of membrane physiology that is precluded by the even more reductionist approach represented by synaptosomal preparations (e.g. Nicholls & Åkerman, 1981; Nachshen, 1985; Rasgado-Flores & Blaustein, 1987).

In this study, neurones isolated from mouse dorsal root ganglia (DRGs) were used as a model system because: (i) the limited cell types in the ganglia express the major voltage-gated currents described in mammalian neurones; (ii) the soma response to metabolic blockade might give insight into the presynaptic basis for synaptic failure. It is widely assumed (if only for want of evidence to the contrary), that the electrophysiological properties of the somatic membranes are similar to those of the terminal membranes, which are not accessible for study; (iii) the cells are spherical and lack processes. Compounds introduced into the cell with a patch pipette are more likely to permeate the cell cytoplasm than in cells that have processes along which diffusion is slow; and (iv) the cells do not have synaptic terminals on the soma, so that responses to the various manipulations described below cannot be due to altered release of transmitters from boutons that remain attached after dissociation.

A preliminary account of some of these data has been published (Duchen & Somjen, 1988).

METHODS

Cells were obtained as previously described (Duchen & Pearce, 1989; Duchen, Valdeolmillos, O'Neill & Eisner, 1990). Mice were killed by decapitation. After a ventral laminectomy (see Biscoe & Duchen, 1986) the lumbar dorsal root ganglia were removed into a saline-containing collagenase type II (Sigma). The composition of the saline was (mM): NaCl, 130; NaHCO$_3$, 26; KCl, 3·0; KH$_2$PO$_4$, 1·25; MgCl$_2$, 2·0; D-glucose, 10. The ganglia were incubated for 30 min at 35 °C, continuously supplied with 95% O$_2$–5% CO$_2$. They were then removed into a similar saline but containing papain (Worthington, 0·035%), cysteine (175 µg/ml, Sigma) and 2 mM-CaCl$_2$, and incubated at 35 °C for at least a further 30 min. Cells were prepared by trituration of a ganglion with fire-polished Pasteur pipettes, in a HEPES-buffered saline (as above, but bicarbonate replaced by NaCl, and with 7·5 mM-HEPES, pH 7·3). The cells generally remained viable for about 2 h and were then replaced by trituration of another ganglion.

Whole-cell patch-clamp recordings were made using standard techniques (Hamill, Marty, Neher, Sackmann & Sigworth, 1981; Duchen, Caddy, Kirby, Patterson, Ponte & Biscoe, 1988). A List EPC7 amplifier was used in combination with a microcomputer, which was used for the generation of voltage-clamp protocols and on-line digital storage (p-clamp, Axon Instruments). Data were also stored on FM tape (Racal, Store-4D), where appropriate. Pipettes were pulled from thin-walled glass, to tip diameters of 2–3 µm, giving resistances of 1–3 MΩ. Series resistance, membrane capacitance and input resistance were routinely determined by analysis of the capacitative transient response to a 20 ms, 10 mV hyperpolarizing command from a holding potential of −60 mV, as no voltage-gated currents are activated by such a step. Series resistance averaged 3 MΩ, ensuring reasonable access of the pipette contents into the cytoplasm. Correction for the voltage-clamp error introduced by the series resistance was calculated and correction made on *I–V* curves when the error was more than 5 mV. Current variance was measured from the current signal filtered between 0·5 and 500 Hz (8-pole Butterworth filters, Barr & Stroud) using a home-made analog standard deviation meter. Moving averages of the standard deviation and of the original, unfiltered signal were then used to calculate variance and mean current.

In early experiments, pipettes were filled with a solution containing (mM): KCl, 130; ethyleneglycol-bis-(β-aminoethylether)*N,N,N'N'*-tetraacetic acid (EGTA), 11; CaCl$_2$, 1·0 (pCa, 8); HEPES, 7·5; pH adjusted to 7·2–7·3 with KOH. Subsequently, the Ca^{2+} buffer used was varied, using: (i) no EGTA, no added Ca^{2+}; (ii) 0·5 mM-EGTA and (iii) 10 mM-1,2-bis(2-amino-phenoxy)ethane-*N,N,N',N'*-tetraacetic acid (BAPTA). When studying Ca^{2+} currents, K$^+$ currents were blocked by using a combination of 105 mM-CsCl$_2$ and 25 mM-tetraethylammonium (TEA) chloride to replace KCl, and 1 µM-tetrodotoxin (TTX, Sigma) was added to the bath to block the TTX-sensitive Na$^+$ current. To prevent run-down of the Ca^{2+} current, MgATP (5 mM) was added to the filling solution. In some other experiments, any of the following were also added to the filling solution: MgCl$_2$, 2 mM; MgATP, 2–5 mM; creatine phosphate, 2 mM; creatine phosphokinase (CPK), 20 units/ml; MgADP, 2 mM; and leupeptin, 100 µM (all from Sigma). Drugs were applied by pressure ejection from a second patch pipette placed close to the cell, and included NaCN (2 mM), carbonyl cyanide *p*-trifluoromethoxyphenyl hydrazone (FCCP; 5 µM), iodoacetic acid (IAA; 200 µM) (all from Sigma) and ionomycin (2–5 µM) (Calbiochem). All experiments were performed at room temperature (18–22 °C).

The data presented were derived from recordings made from several hundred cells. For each group of experiments, data were obtained from at least ten cells and usually more.

RESULTS

All the manipulations used to inhibit metabolism – application of CN$^-$, removal of glucose, inhibition of glycolysis with IAA or application of the mitochondrial uncoupler FCCP – routinely hyperpolarized cells and reduced their excitability. Qualitatively similar responses were seen in large and small cells, despite their electrophysiological differentiation (see, for example, Harper & Lawson, 1985; Duchen & Pearce, 1989). On the assumption that it would maximize the responses, CN$^-$ was initially applied in a glucose-free solution. In practice, this in fact made
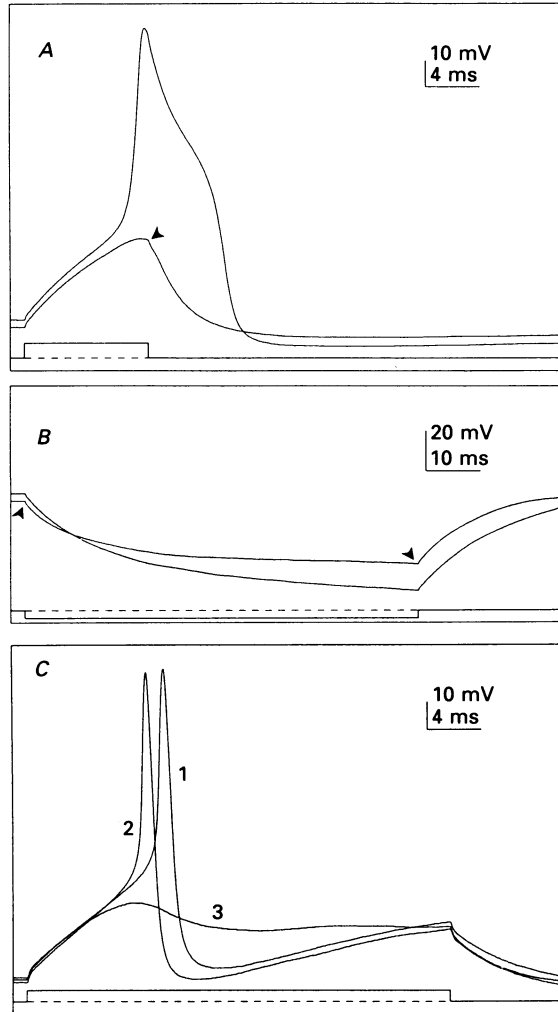
Fig. 1. Whole-cell recordings made under current-clamp control. *A*, a short 300 pA depolarizing step evoked a prolonged action potential from a small cell. 2 mM-CN^- in glucose-free saline (arrows) hyperpolarized the cell and the pulse failed to elicit an action potential. *B*, the electrotonic response to a longer, hyperpolarizing 300 pA step applied to the same cell was reduced by CN^- (arrows). The cell resting potential was -58 mV. *C*, recordings from a larger (diameter *circa* 35 μm) cell in response to a 220 pA depolarizing step (labelled 1). This cell generated a faster action potential which was followed by an after-hyperpolarization. Ten seconds after application of CN^-, the threshold for the action potential was shifted in the hyperpolarizing direction and the after-hyperpolarization was increased (trace 2). After CN^- had been present for 30 s, the step failed to elicit an action potential. The cell membrane potential was -72 mV.

little difference, and either CN^- or zero glucose alone had similar effects to the combination. FCCP and IAA had similar effects to CN^- and to each other (see below) but proved less readily reversible, so that CN^-, with or without glucose, was used for the majority of experiments illustrated. The characteristic electrophysiological

responses seen under current-clamp control will first be described. This will be followed by a voltage-clamp analysis of the underlying conductance changes.

Recordings under current-clamp control

Under whole-cell recording conditions in current clamp, spontaneous activity was unusual. In order to examine the effect of a combination of CN^- and glucose withdrawal on cell excitability, depolarizing steps were applied close to the threshold for the action potential (Fig. 1). The record shown in Fig. 1A shows the long-duration action potential recorded from a subpopulation of (small, i.e. diameter *circa* 20 μm, capacitance < 25 pF) sensory neurones in response to a short depolarizing step. In response to CN^- applied in glucose-free saline, cells hyperpolarized, and the depolarizing current step in this example was no longer sufficient to elicit the action potential.

The response to a hyperpolarizing current step, which was not large enough to activate the inwardly rectifying current I_H (see below) and therefore shows only the charging of the cell impedance, is shown in Fig. 1B. During exposure to CN^- and zero glucose, the membrane potential hyperpolarized and the electrotonic voltage response was reduced, demonstrating an increase in membrane conductance.

In addition to this increase in conductance, the after-hyperpolarization that follows action potentials was exaggerated in the presence of CN^-, as shown in Fig. 1C. These records come from a larger cell (*circa* 35 μm diameter, capacitance *circa* 50 pF) which exhibited a faster action potential than the cell illustrated above, showing that the nature of the response was essentially the same in different classes of cells within the preparation. A long depolarizing step was used to excite an action potential. The first response following the application of CN^- shows an apparent reduction in the threshold for the action potential, and an increase in the amplitude of the after-hyperpolarization. During the next depolarizing step, the membrane was shunted.

Recordings under voltage-clamp control

The ionic basis of the increased resting conductance was determined by experiments under voltage-clamp control. Application of CN^- (Fig. 2) increased an outward current which was seen most readily if the cell membrane potential was held at or positive to -50 mV. The outward current was associated with an increase in current fluctuations or noise, as seen in the high-pass-filtered record shown in the middle trace in Fig. 2, indicating that the current was due to an increase in the opening probability of ion channels (rather than an altered pump current, for example). The lowest trace shows the standard deviation of the current derived from the high-pass-filtered trace. These data were used to calculate current variance as shown below (see Fig. 7).

The current voltage (I–V) relation of the CN^--induced outward current was studied by using hyperpolarizing voltage ramps from -50 to -150 mV (200 ms peak to peak) to sample the current over that voltage range before, during and after application of CN^- (Fig. 3A). In this instance, the rate of the ramp was chosen to allow sampling of the resting conductance with minimal activation of the voltage-gated inward current, I_H (see below). The resting potential of the cell (the potential

at which no net current flows) hyperpolarized in the example illustrated from about -74 to -82 mV. The *I–V* curve of the CN^--induced current (Fig. 3*B*) was obtained by the digital subtraction of the control response from that obtained during the developed outward current. The current reversed between -85 and -90 mV, very close to the predicted E_K of -88 mV, and shows slight outward rectification. FCCP
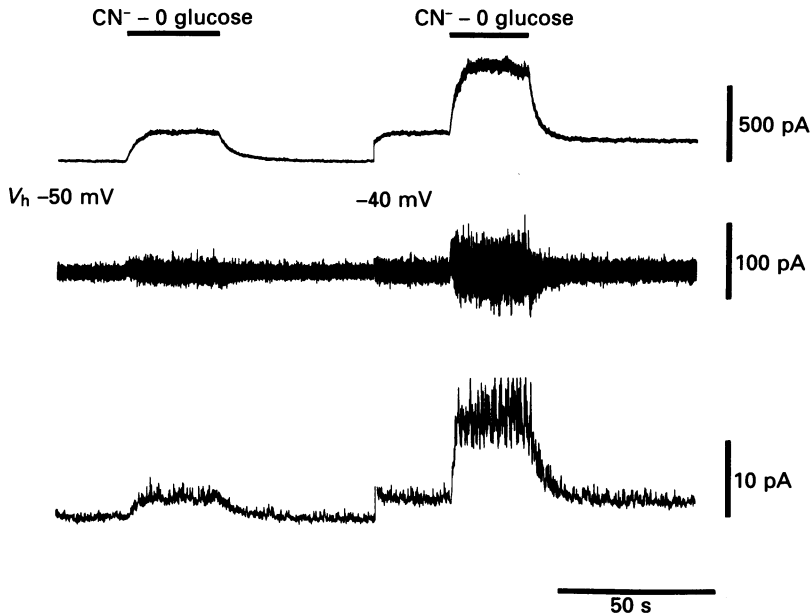

Fig. 2. Recordings made from a large cell (diameter about 40 μm) under voltage-clamp control. The membrane potential was clamped initially at -50 mV. 2 mm-CN^- applied in glucose-free saline induced an outward current associated with increased current fluctuations, seen more clearly in the lower traces. The middle trace shows the current filtered between 0·5 and 500 Hz. This signal was then processed by an analog circuit to show the standard deviation from the mean (bottom trace). The resting outward current, the response to CN^- and the associated noise were all increased when the cell membrane potential was clamped at -40 mV.

(Fig. 4), glucose removal and IAA (not shown) increased a conductance with similar characteristics, except that the response to FCCP typically outlasted the period of application by several minutes. As shown in Fig. 4*A*, FCCP similarly hyperpolarized the resting membrane potential, in the example shown from -73 to -78 mV, and the FCCP-induced current (Fig. 4*B*) reversed close to -90 mV.

Thus, close to the cell resting potential, blockade of electron transport by CN^-, glucose removal, inhibition of glycolysis with IAA and reduction of the mitochondrial membrane potential with FCCP (Heinonen, Åkerman & Kaila, 1984) each increases a K^+ conductance, or g_K. Potassium was the only ion present with a negative reversal potential under these recording conditions, and the outward current was not seen when K^+ currents were blocked by replacement of K^+ in the pipette with Ca^+ and TEA^+.
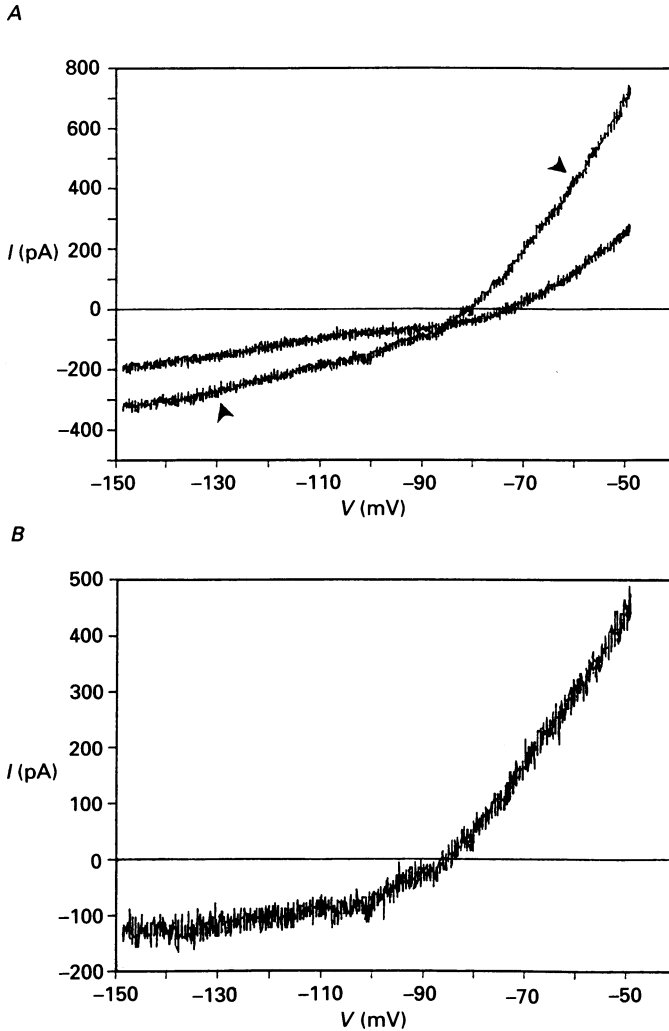
A

B

Fig. 3. *A*, the *I–V* relation of the current induced by CN^-, obtained by passing a hyperpolarizing ramp from the holding potential of -50 mV to -150 mV before and at the peak of the response to CN^- (arrows). The increased outward current at -50 mV reversed at about -85 mV. *B* shows the *I–V* curve of the CN^--evoked current obtained by subtraction of the control record from that obtained in the presence of CN^-.

Potassium channels carrying the current

There are two major candidates for this role: (i) Ca^{2+}-dependent potassium channels. We have shown (Biscoe, Duchen, Eisner, O'Neill & Valdeolmillos, 1988; Duchen *et al.* 1990) that intracellular Ca^{2+} concentration ($[Ca^{2+}]_i$) rises in DRG cells in response to CN^-, glucose removal or FCCP. (ii) ATP-regulated K^+ channels, a population of channels present in cardiac myocytes (Noma, 1983), pancreatic β-cells (Cook & Hales, 1984), skeletal muscle (Castle & Haylett, 1987) and probably in

some CNS neurones (Bernardi, Fosset & Lazdunski, 1988) that are kept closed by ATP and which open as ATP levels fall.

Addition of 5 mM-MgATP to the pipette-filling solution, which would be expected to keep ATP-dependent channels closed, made no difference to the response to CN^-
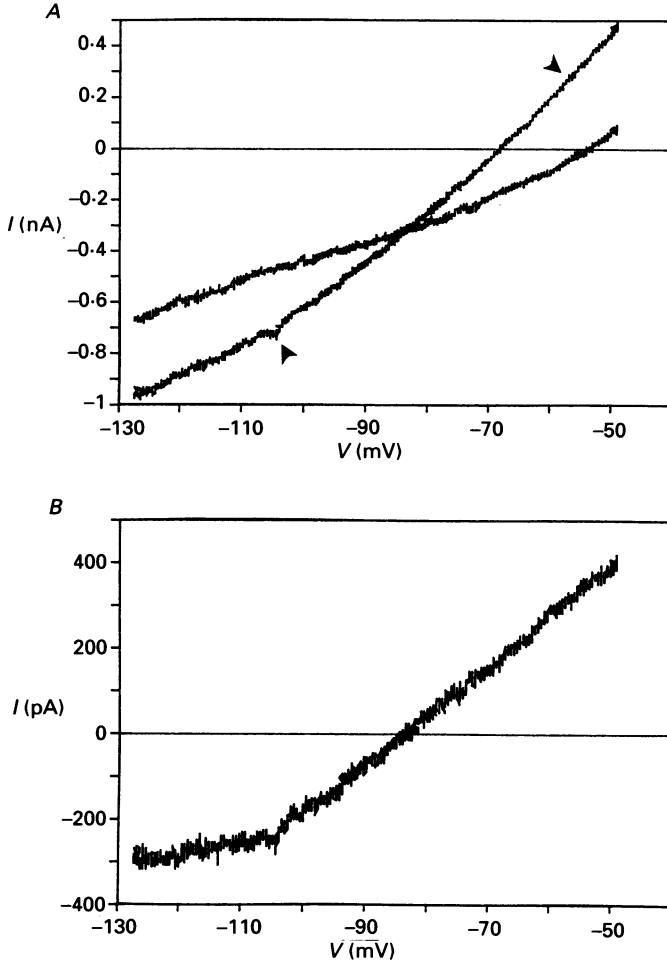

Fig. 4. *A*, the *I–V* relation of the current induced by 5 μM-FCCP. The current reversed at about -85 mV and showed a degree of outward rectification, seen more clearly in the subtracted records shown in *B*.

or to FCCP. As the ATP/ADP.P_i ratio is more important in determining the free energy available to the cell than the absolute concentration of intracellular ATP in the cytoplasm, creatine phosphate (CP), creatine phosphokinase (CPK), Mg^{2+} and MgATP were included in the pipettes in some experiments to rephosphorylate ADP. These agents again did not make any difference to the response (Fig. 5*A* and *B*). Addition of 2 mM-ADP to the pipette, which might be expected to diffuse into the

cell and lower the $ATP/ADP.P_i$ ratio, also had no apparent effect on either the resting membrane conductance or on the responses to metabolic blockade. The addition of MgATP or CP/CPK/ATP did dramatically reduce the rate of run-down of the Ca^{2+} currents and had independent effects on the GABA-gated chloride current (Duchen, 1989), suggesting that access of the agents to the cytoplasm was not restricted, although it is impossible to be absolutely sure that sufficient ATP was available throughout the cell.
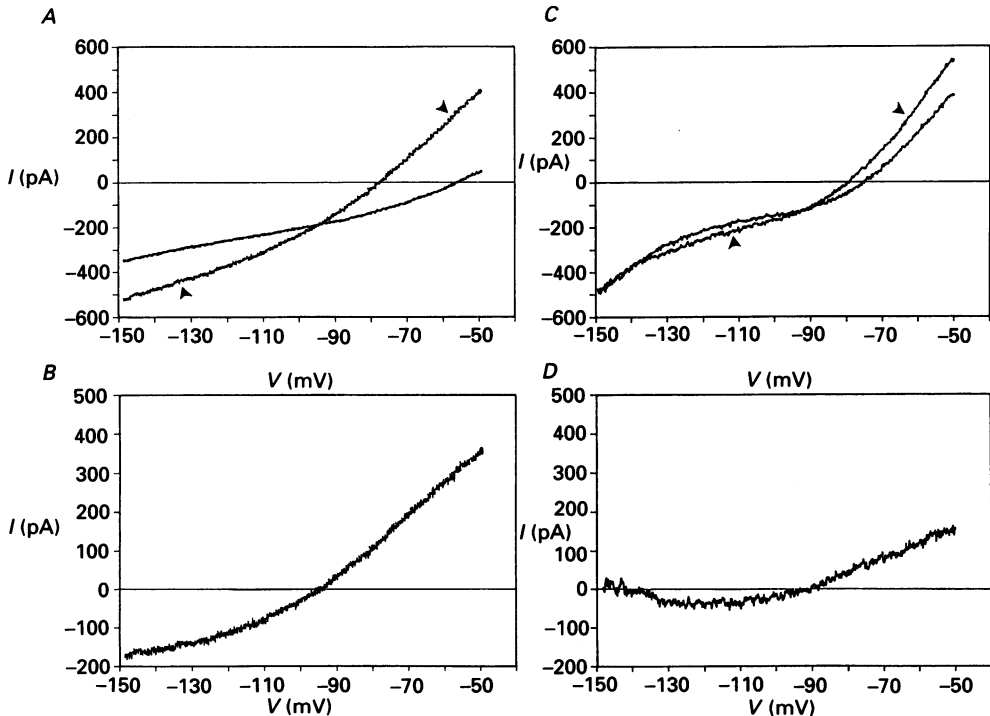

Fig. 5. The current evoked by CN^- was examined under different recording conditions. In A and B, 0·5 mM-EGTA, 5 mM-MgATP, 2 mM-creatine phosphate, and 20 units/ml CPK were added to the pipette-filling solution. CN^- increased an outward current at -50 mV which reversed close to -90 mV, and showed outward rectification. The records shown in C and D were obtained from a cell bathed in Ca^{2+}-free saline (including 1 mM-EGTA). CN^-, applied in Ca^{2+}-free saline, evoked a small outward current which reversed close to -90 mV. Note that a slower ramp (500 ms peak to peak) was used to obtain these data. The inward inflexion on the control trace at hyperpolarized potentials is due to activation of I_H (see below).

When the rate of intracellular Ca^{2+} buffering was increased, by using 10 mM-BAPTA, the responses in many cells were smaller than expected (i.e. less than 100 pA at -50 mV), but larger responses were still seen in some cells. If Ca^{2+} buffering was reduced, using only 0·1 mM-BAPTA or 0·5 mM-EGTA, large (> 250 pA at -50 mV) responses were routinely seen (such as those illustrated above). However, these results remained equivocal, probably reflecting the inadequacy of control over intracellular Ca^{2+} buffering by the pipette contents in these relatively large cells. However, when cells were incubated in a Ca^{2+}-free solution, responses to

CN^- were abolished in most cases. Under these conditions, CN^- did occasionally induce a small outward current (Fig. 5C and D) which reversed at E_K. In these instances, however, the current was not associated with a clear increase in membrane noise, suggesting that a component of the current may be carried through a channel of very low conductance.
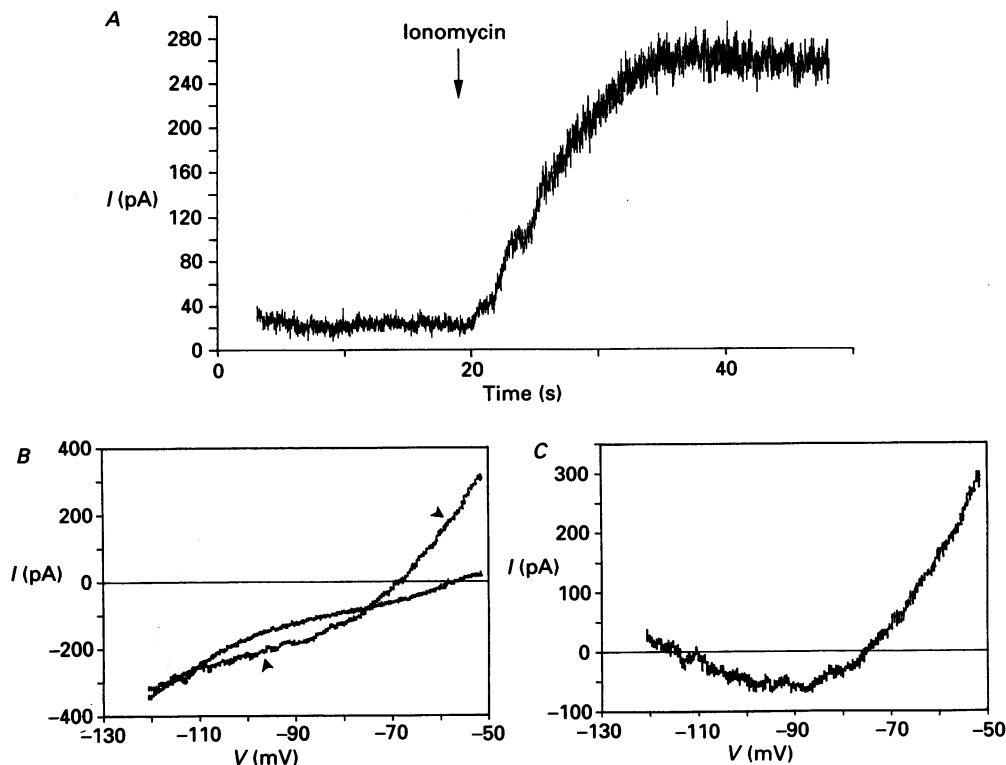

Fig. 6. A, a brief application of ionomycin (5 μM; arrow) to a cell clamped at a potential of -50 mV initiated a long-lasting outward current associated with an increase in membrane fluctuations. B and C show I–V relations of the current evoked by ionomycin (arrows). The current reversed at about -75 mV, and hyperpolarized the resting potential by about 15 mV. As in Fig. 5C and D, a slower ramp was used, and activation of I_H at hyperpolarized potentials can be seen in the control trace. Reduction of I_H (see below) after the application of ionomycin accounts for the upward curve on the record shown in C.

The Ca^{2+}–H^+ ionophore, ionomycin (Liu & Hermann, 1978), which should raise $[Ca^{2+}]_i$ without affecting free-energy availability directly, induced a very similar increase in g_K. Figure 6A shows that application of 5 μM-ionomycin increased an outward current at -50 mV associated with an increase in noise. The I–V curves before and after application of the ionophore are shown in Fig. 6B, and the I–V curve of the ionomycin-induced current in Fig. 6C. The resting membrane potential in this cell hyperpolarized from -58 to -70 mV in response to ionomycin. These responses were again most clearly seen if the pipette Ca^{2+} buffering capacity was kept low (either zero EGTA, no added Ca^{2+} or 0·5 mM-EGTA only). The responses to

ionomycin under these conditions were only reversible if the pipette-filling solution contained strong Ca^{2+} buffers. In some cells, the reversal potential for the current evoked by ionomycin was slightly positive to E_K (at about -70 to -80 mV). With repeated applications, the outward current gave way to a net inward current, and the
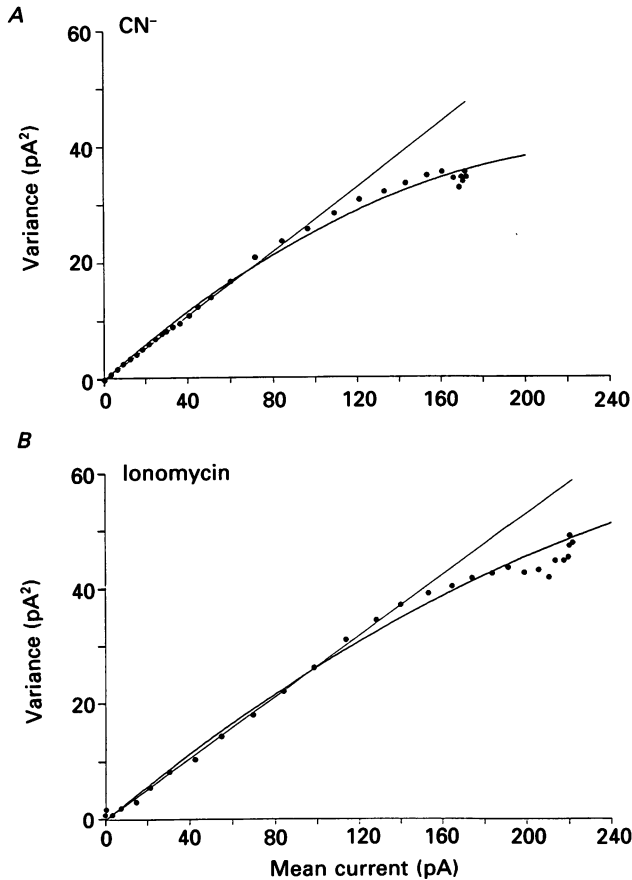

Fig. 7. Analysis of current variance evoked by CN^- (*A*) and by ionomycin (*B*) in two different cells at a holding potential of -50 mV. The responses to CN^- during the onset and offset of the response have been averaged. As the response to ionomycin was irreversible, the variance during the onset of the response only is plotted. The variance increases directly as a function of the mean current according to the equation quoted in the text. A straight line was fitted to points < 80 pA in *A* and < 100 pA in *B*, giving slopes (*i*) of 0·28 and 0·265 pA respectively ($R^2 > 0.95$). Values for *i* of 0·32 and 0·29 were required to obtain adequate fits for the parabolic function $\sigma^2 = iI_m(1-p_0)$, however (see text).

reversal potential of the response moved positively, suggesting a contribution to the net current from other Ca^{2+}-activated cationic or chloride channels. This typically preceded the development of a large noisy leakage current and an end to the recording.

Noise fluctuation analysis of the whole-cell currents was used to compare the mean conductance of the channels carrying the current induced by CN^- and by ionomycin. Figure 7 shows the analysis of current variance in relation to the mean outward
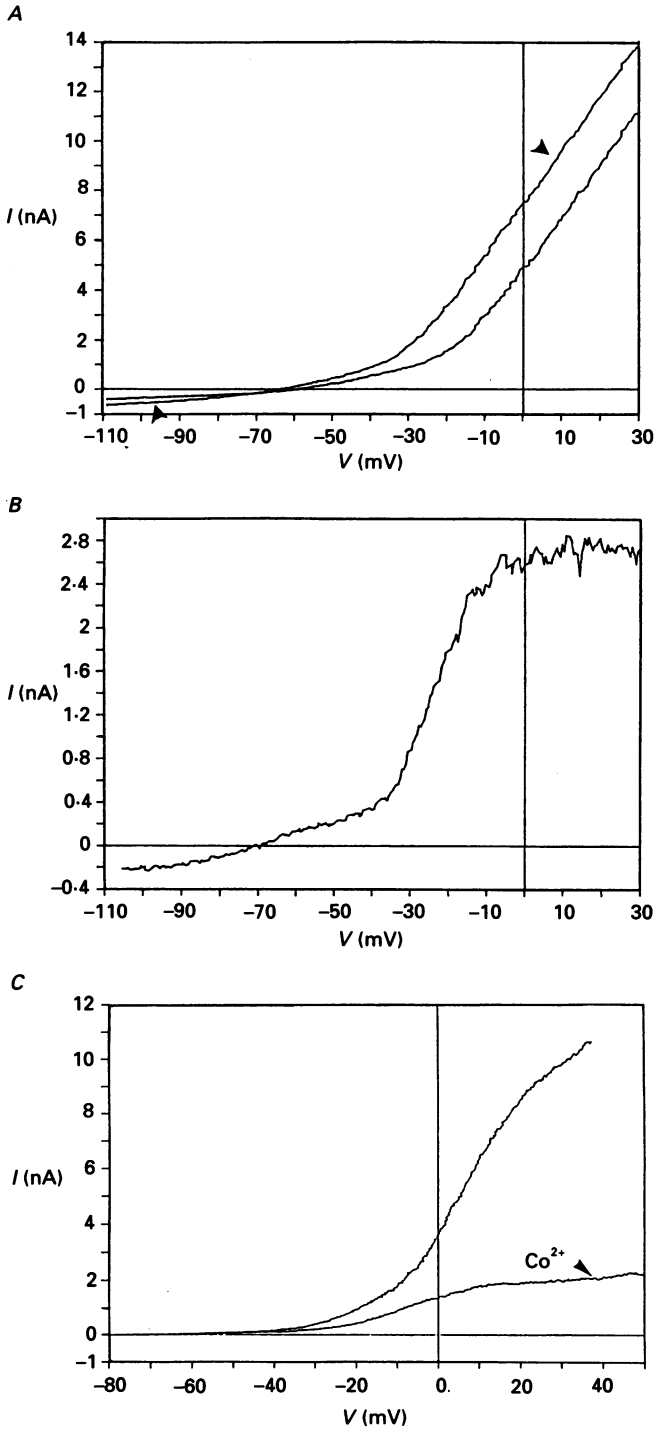
A

I (nA)

V (mV)

B

I (nA)

V (mV)

C

I (nA)

Co²⁺

V (mV)

Fig. 8. For legend see facing page.

current developed at -50 mV in response to CN^- (A) and to ionomycin (B). The increasing variance and current during the onset (for both drugs) and the decreasing values during the offset (for CN^- only) of the responses have been averaged. The variance (σ^2) is related to the mean current I_m by the equation: $\sigma^2 = I_m i (1 - p_0)$, where i is the mean single-channel current, and p_0 is the probability of channel opening. When p_0 is very small, $i = \sigma^2/I_m$. The mean single-channel conductance, estimated from the slope of the linear regression line, was similar in response to both CN^- (9.14 ± 1 pS, $n = 6$) and to ionomycin (9.3 ± 0.3 pS, $n = 3$). Only cells in which the response reversed clearly at E_K were used for this analysis to avoid contributions from either Ca^{2+}-activated Cl- (see below) or cation channels.

In Fig. 7, both the linear regression lines fitted through the points over the range below 80 pA in A and 100 pA in B and parabolas fitted by the above equation have been plotted. Although the linear regression lines fitted the data with a correlation coefficient (R^2) of > 0.99, in order to fit the parabolas, the estimate for i had to be significantly greater than the value given by the slope of the line, giving estimated conductances for these examples closer to 10 pS (see figure legend). The parabolic functions could only be satisfactorily fitted if the current at which $p_0 = 0.5$ could be estimated, and this analysis could therefore only be applied to the examples shown. For these data, this was 250 pA for CN^- (Fig. 7A) and 320 pA for ionomycin (Fig. 7B). This would mean that the maximum current for these cells (i.e. when $p_0 = 1$) was 500 and 640 pA respectively, giving an estimate of a total number of approximately 2000 channels per cell.

It remains likely, however, that the current is carried by more than one class of channel, as a small current was seen in response to CN^- in the absence of external Ca^{2+} that was not associated with an obvious increase in noise. If the contribution of this component to the net current is significant, this would result in a substantial underestimate of the single-channel conductance of the channel generating the noise. These measurements are thus useful primarily for comparative purposes, and direct measurements of the single channels are required to determine their properties.

Changes in Ca^{2+} buffering by CN^-

When a larger depolarizing voltage ramp was used to sample currents over the range from -110 to $+30$ mV, the form of the I-V relation for the increased g_K was seen to be more complex than indicated above. Figure 8A shows the responses to such a ramp before and during application of CN^-, while Fig. 8B shows the CN^--

---

Fig. 8. A shows the I-V relation of the CN^--activated current (arrows) over the range -110 to $+30$ mV, shown in B after subtraction of responses before from those during CN^-. An increased conductance close to the resting potential reversed at about -75 mV. In addition, a sharp increase in the outward current was seen above -35 mV reaching a plateau between -10 and $+10$ mV. The plateau is the range of peak voltage-gated Ca^{2+} entry (see below), and the inflexion is close to the threshold for the high-threshold Ca^{2+} current. Blockade of voltage-gated Ca^{2+} entry by 2 mm-cobalt (C) reduced a large proportion of the outward current generated in response to such ramps, showing the component of the outward current carried by Ca^{2+}-dependent K^+ channels activated by voltage-gated Ca^{2+} entry. Because the outward currents are very large, compensation for the correspondingly large voltage error has been made in plotting these data.

induced current obtained by subtraction. In response to CN^-, there is an increased conductance around the resting potential, reversing at about -75 mV, but also a sharp increase in conductance appearing above -35 mV. This is the threshold for the high-threshold Ca^{2+} currents (see below). Activation of the Ca^{2+} current raises $[Ca^{2+}]_i$, activating $g_{K(Ca)}$, which will represent a component of the outward current
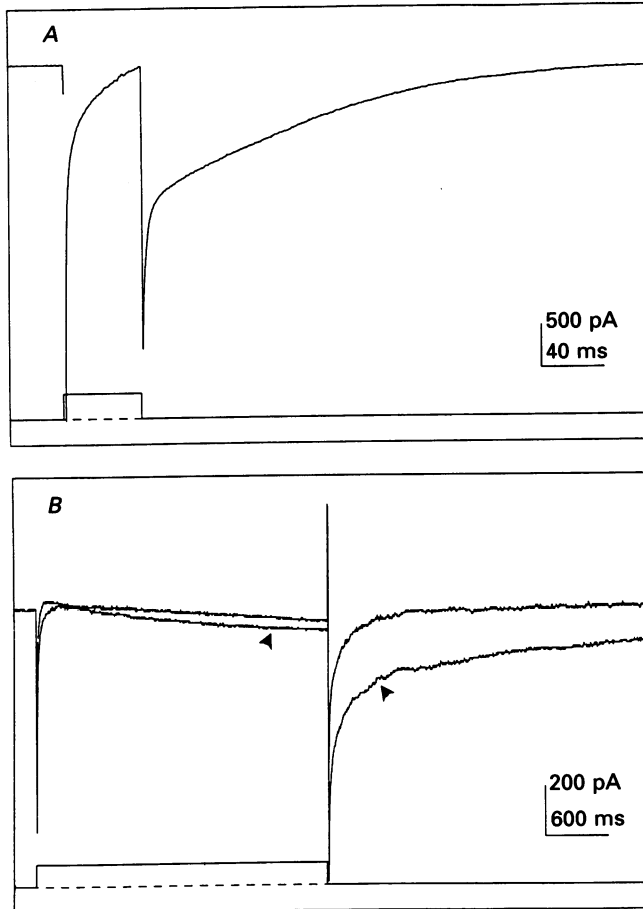

Fig. 9. *A*, in this cell, a step to -10 mV from a holding potential of -70 mV evoked an inactivating inward Ca^{2+} current followed by a prolonged inward tail current on stepping back to -70 mV. *B*, later in the recording from the same cell, the inward current had largely washed out, but a prolonged depolarizing step still evoked an inward tail, now much reduced. Application of CN^- (arrows), however, increased both an inward current at -10 mV, and the inward tail current.

seen in response to the ramp. This is illustrated by the reduction in the outward current seen in the presence of 2 mM-cobalt (Fig. 8*C*). The effect of CN^- on the response is again best explained if the CN^- reduces the ability of the cell to remove from the cytoplasm the Ca^{2+} brought in by the depolarization, so that, on activation of the Ca^{2+} current by depolarization, the CN^--induced increase in outward current is exaggerated. This could account for the increased after-hyperpolarization seen in the presence of CN^- (Fig. 1*C*).

A small number of cells showed very pronounced slowly inactivating inward tail currents following depolarizing steps (Fig. 9A). The current most probably reflects the activation of a Ca^{2+}-dependent Cl^- conductance (Mayer, 1985) as it has properties which closely resemble descriptions of that conductance. It was blocked by Ca^{2+} channel blockers, reversed at E_{Cl} (0 mV under these recording conditions) and
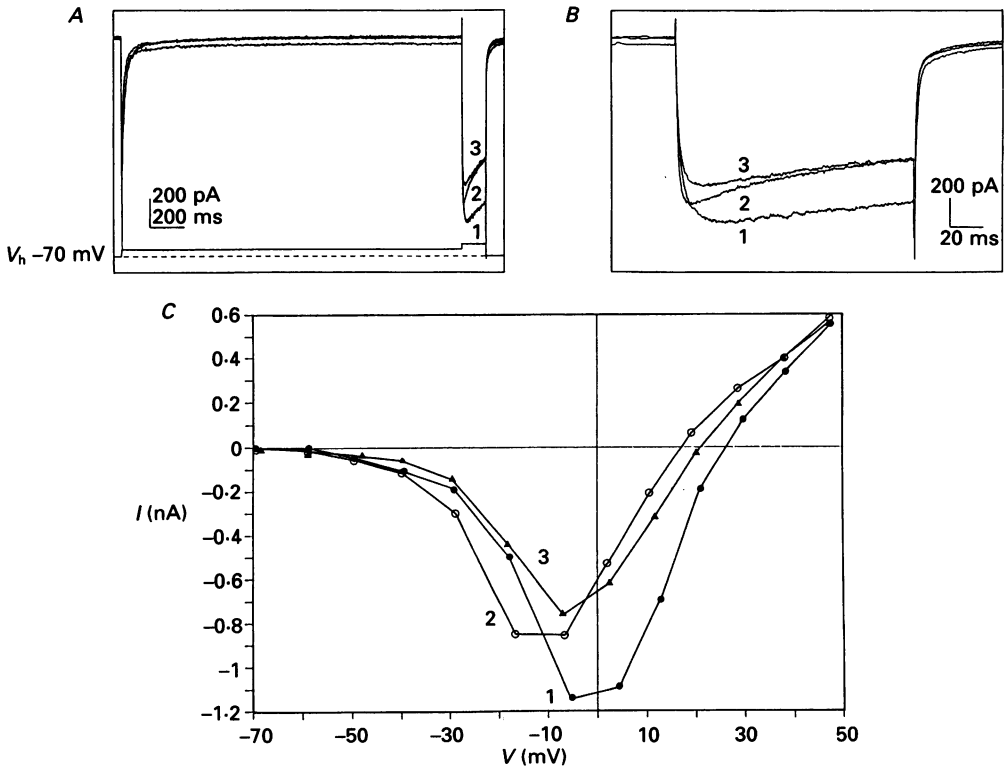

Fig. 10. Effects of CN^- on the high-threshold Ca^{2+} current. *A*, a conditioning step to -35 mV for 2 s preceded the test step to $+10$ mV. The responses at $+10$ mV are shown in greater detail in *B* showing the high-threshold Ca^{2+} current before (1), during (2) and after (3) application of CN^-. CN^- reduced the amplitude of the current and increased the rate of inactivation at this test potential. While the rate of inactivation recovered to control values, the amplitude of the current did not. The *I–V* curves for the current are shown in *C*, showing the shift of the activation curve for the current in the hyperpolarizing direction from the control (●, 1) in the presence of CN^- (○, 2) and the long-lasting reduction in the peak current (▲, 3). The records in *A* and *B* are each the average of four responses before, during and after application of CN^-.

showed the characteristically very slow inactivation. The current was seen only occasionally. It therefore proved difficult to study systematically, and could theoretically also result from a Ca^{2+}-activated non-selective cation conductance. CN^- increased the amplitude and duration of the tail current (Fig. 9B), despite reduction in the Ca^{2+} current itself (see below).

These findings are again consistent with impaired removal of the Ca^{2+} load imposed by depolarization, increasing activation of the channels carrying the tail current.

Effects of CN⁻ on calcium currents

One of the major effects of metabolic impairment in the CNS is the failure of synaptic transmission. As it has been suggested previously that this is a predominantly presynaptic phenomenon (Hansen *et al.* 1982; Adams, Takeda & Umbach, 1985), the Ca^{2+} currents which presumably underlie the control of
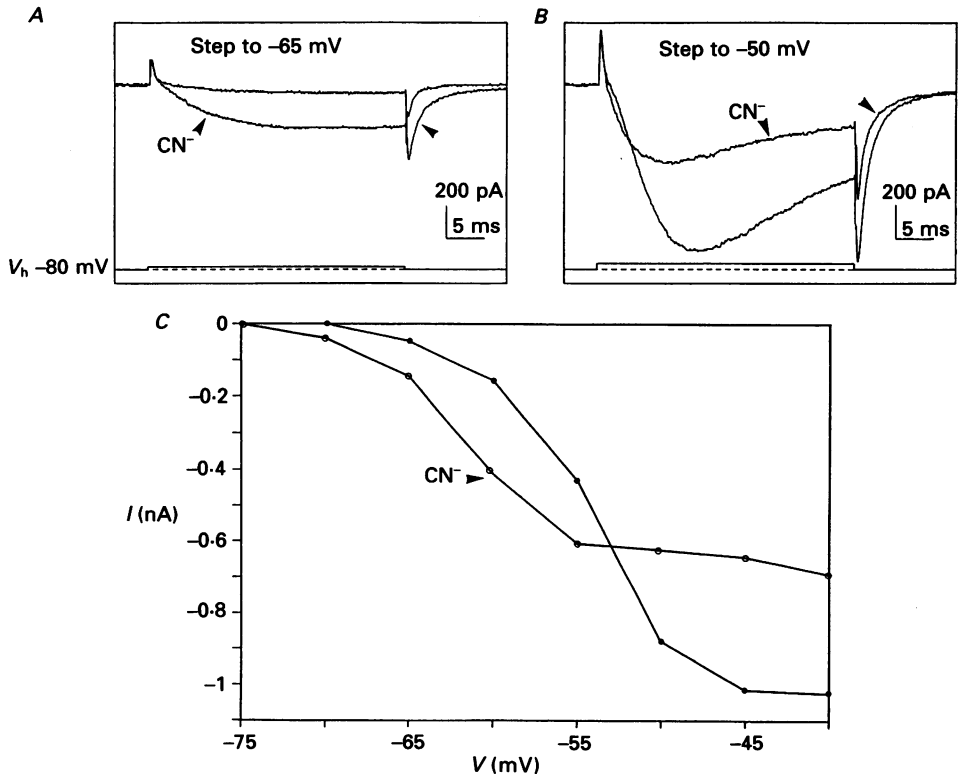

Fig. 11. Effect of CN⁻ on the low-threshold Ca^{2+} current. Incrementing depolarizing steps from a holding potential of -80 mV activated the current. *A*, a step to -65 mV activated a very small inward current at -65 mV, which was clearly increased by CN⁻ (arrows). *B*, a step to -50 mV evoked an almost maximal conductance, which was markedly reduced by CN⁻ (arrows). The *I–V* relations for the current before (●) and during (○) CN⁻ are shown in *C*. The activation range for the current hyperpolarized by 5–8 mV, and the peak current was reduced. The response was almost completely reversible.

transmitter release were studied. At least two classes of Ca^{2+} current may be identified in these cells: a low-threshold inactivating current, now commonly referred to as a T current, and high-threshold currents, now usually referred to a L and N (Nowycky, Fox & Tsien, 1985). Differentiation between N- and L-type currents is difficult in whole-cell recordings, as depolarizing steps from holding potentials negative to -70 mV evoke both T- and L-type currents which summate, suggesting the presence of an activating component. The currents will therefore be referred to only as high and low threshold. Study of the Ca^{2+} currents in the present context is

further complicated by the phenomenon of run-down. Unless ATP and Mg^{2+} were included in the pipette-filling solution, the high-threshold Ca^{2+} current rapidly attenuated, and could therefore not be studied. It seems obvious therefore that a large fall in ATP will lead to a reduction in the amplitude of the Ca^{2+} current. However, failure of synaptic transmission seems to occur before levels of ATP have fallen significantly (Cox, Morris, Feeney & Bachelard, 1983; Bachelard, Cox, Feeney & Morris, 1985), so the effects of CN^- and/or zero glucose on the currents were examined with the inclusion of MgATP in the pipette to reduce the rate of run-down.

The peak current carried by both the low-threshold and high-threshold conductances was irreversibly attenuated following brief applications of CN^-.

To examine the high-threshold current separately, conditioning depolarizing steps to -35 mV were applied for 2 s to allow full inactivation of the low-threshold current and of any TTX-insensitive Na^+ current (Fig. 10A). A subsequent step to $+10$ mV was used to test the slowly inactivating high-threshold current. CN^- increased the rate of inactivation of the current and decreased its peak amplitude (Fig. 10B) in all cells tested. While the rate of inactivation of the current returned to control values, the amplitude of the current usually remained reduced. The I–V relation for the high-threshold current before, during and after application of CN^- is shown in Fig. 10C. The threshold for the current was shifted in the hyperpolarizing direction during application of CN^-, returning to the control range on its removal, although the peak current remained reduced. Addition of leupeptin to the pipette-filling solution made no apparent difference to the response to metabolic blockade.

Figure 11 shows the response of the low-threshold current to CN^-. Again, the threshold was shifted in the hyperpolarizing direction by CN^-, so that the current could appear to increase if test steps were close to the threshold (Fig. 11A and C), although the peak current was clearly reduced (Fig. 11B and C). The degree of reversibility of the response was more variable than with the high-threshold current, and typically at least partial recovery was seen.

Metabolic blockade and raised $[Ca^{2+}]_i$ also block I_H

Large cells ($> 30 \mu$m diameter) in this preparation express an inward current which is activated by hyperpolarization, called I_H by Mayer & Westbrook (1983). The current activates over 100–200 ms in response to steps to potentials negative to -70 mV and is non-inactivating.

When repeated steps from -50 to 110 mV were applied during the application of CN^-, FCCP, IAA or ionomycin, an increased outward current was seen at the holding potential, and an increased inward current was seen immediately on stepping to -110 mV (Fig. 12A), reflecting the increased resting g_K discussed above (Figs 2–4). The time-dependent I_H, however, was clearly reduced by either the inhibitors or by ionomycin in all cells tested ($n > 30$). This is seen in the I–V curve shown in Fig. 6B and C, where a slower ramp was used than in Figs 3 and 4. During the control ramp from -50 to -120 mV, an inward inflexion is seen on the current response which is absent during the response after application of ionomycin. This is the basis for the otherwise curious upward inflexion on the difference curve at very negative potentials seen in Fig. 6B (also seen in Fig. 5D). On removal of the metabolic inhibitors, the resting current and instantaneous response to the step gradually
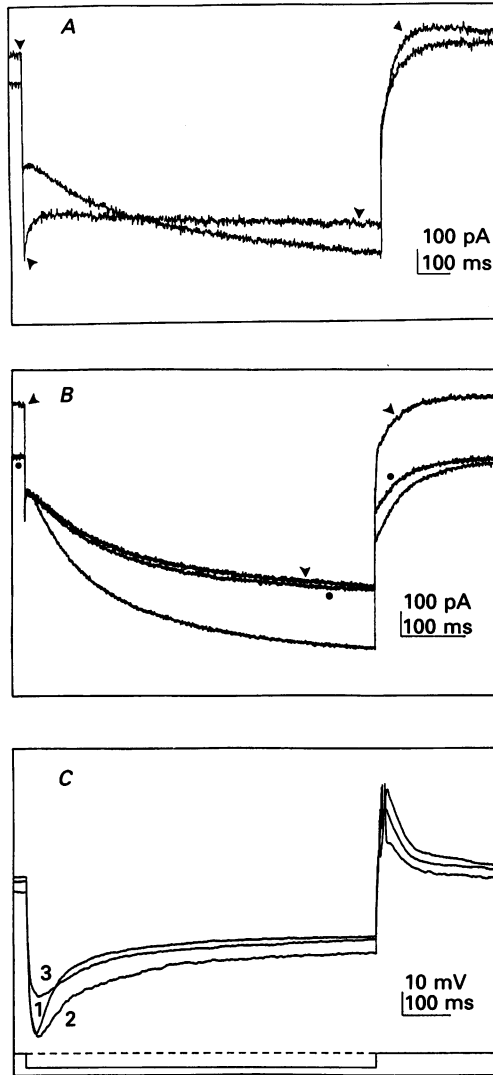
Fig. 12. Effects of CN^- on I_H. *A*, steps from -50 to -100 mV activated a slowly developing inward current. CN^- (arrows) increased both an outward current at -50 mV, and the instantaneous inward current in response to the step at -100 mV, reflecting the increased resting conductance. The slowly developing inward current was much reduced, however. *B*, the loss of I_H was largely irreversible. Three traces are shown in response to a step from -50 to -90 mV, the reversal potential of the CN^--induced current. CN^- increased the outward current at -50 mV and reduced I_H (arrows), without changing the instantaneous current at -90 mV. I_H remained reduced (●) after removal of CN^-. *C* shows the consequence of the reduced I_H for the behaviour of another cell in current clamp. The electrotonic response to a 500 pA step shows a hyperpolarization followed by repolarization to an intermediate level (1) due to activation of I_H. CN^- initially (2) appeared to increase the voltage response to the pulse and reduced the repolarizing sag, due to loss of I_H. A later response (3), still in the presence of CN^-, shows more obviously the consequence of the increased conductance in response to CN^-.

returned to control values, but the time-dependent I_H failed to recover. This is illustrated further in Fig. 12B. Steps were applied from -50 mV to the reversal potential of the CN^--induced current, -90 mV. In response to CN^-, an increased outward current was seen at the holding potential (arrows), while only the decreased I_H was seen at -90 mV. On removal of the CN^- (●), the holding current returned to control levels, but I_H remained reduced.

The consequences of these changes in I_H for the behaviour of the cell in current clamp are illustrated in Fig. 12C. Activation of I_H is responsible for the repolarizing sag on the electronic potential in response to a hyperpolarizing current step. On application of CN^-, the electrotonic response appeared to grow larger at the steady state. This could lead to the impression that cell input resistance had increased, while the instantaneous response shown in voltage clamp above shows clearly that it had, in fact, decreased.

DISCUSSION

Even transient disturbances in energy supply to the central nervous system lead to potentially catastrophic changes in CNS function. While it is predictable that energy deprivation will eventually lead to a fall in the $ATP/ADP.P_i$ ratio and consequent alterations in the activity of membrane pumps and transmembrane ionic gradients, the relative rates of these changes and their contributions to altered membrane excitability are less readily predictable. In the present study, some of the processes that may underlie early and potentially reversible alterations in cell function have been identified. Within seconds of the application of metabolic blocking agents, an increased Ca^{2+}-dependent g_K develops which hyperpolarizes the neurones and shunts the membrane. The conductance reflects a rise in resting $[Ca^{2+}]_i$ which results, at least in part, from release from an intracellular compartment (Duchen *et al.* 1990). Calcium-dependent K^+ and calcium-dependent Cl^- currents which are activated by voltage-gated Ca^{2+} entry during depolarization are also enhanced, reflecting impaired intracellular Ca^{2+} buffering. Voltage-gated Ca^{2+} currents are reduced, as is I_H, again as a consequence of raised $[Ca^{2+}]_i$.

These findings suggest that the primary determinant of the early response of a population of neurones to metabolic insult will be the array of membrane channels expressed and the effects of raised $[Ca^{2+}]_i$ on their activity. There exists a family of Ca^{2+}-dependent K^+ channels with variable conductances and with variable voltage and calcium sensitivities (for recent reviews, see Blatz & Magleby, 1987; Latorre, Oberhauser, Labarca & Alvarez, 1989). Variations in the channels expressed in different cells may account for some of the variability in the responses of different neurones to similar stimuli (see, for example, Biscoe & Duchen, 1989). The expression of Ca^{2+}-dependent Cl^- channels will also contribute to the response to raised $[Ca^{2+}]$, differing in different populations of cells according to their treatment of chloride. Dorsal root ganglion cells accumulate Cl^-, and will depolarize following activation of a Cl^--dependent Ca^{2+} conductance, while most central neurones would hyperpolarize (Owen, Segal & Barker, 1984). No evidence for the expression of ATP-dependent channels in DRG neurones has emerged in this study. If such channels are expressed in subpopulations of central neurones (see Bernardi *et al.* 1988) this might be a further basis for the differential sensitivity of neuronal populations to hypoxia.

Some of the effects of metabolic blockade reported here have proved to be irreversible, contrasting with the reversibility of the change in $[Ca^{2+}]_i$ and of the increased $g_{K(Ca)}$ (Biscoe *et al.* 1988; Duchen *et al.* 1990). Some of the alterations in membrane conductances described may reflect activation of Ca^{2+}-dependent enzymes rather than direct effects of Ca^{2+} on channels, leading to irreversible or slowly reversible alterations in channel function. Alternatively, the irreversibility of the responses may be related to the dialysis of cytoplasmic factors required for restoration or maintenance of normal channel function into the patch pipette. Loss of the Ca^{2+} current may be due to the loss of phosphorylating factors (Kostyuk, 1984; Chad & Eckert, 1986) so that after Ca^{2+}-induced block of Ca^{2+} channels (Lee, Marban & Tsien, 1985; Morad, Davies, Kaplan & Lux, 1988) during the metabolic insult, or activation of Ca^{2+}-dependent enzymes that dephosphorylate the channels, the cells lack the mechanisms needed to restore channel function. Closer correlations of altered activity of membrane conductances with $[Ca^{2+}]_i$ and introduction of enzyme-blocking agents into the cytoplasm will be required to answer these questions.

The effect of metabolic inhibitors on I_H was most striking, and also appears to be due to a rise in $[Ca^{2+}]_i$, as it could be affected by ionomycin. This effect of raised $[Ca^{2+}]_i$ on I_H has not been described before. I_H is known to be reduced after peripheral axotomy (Gallego, Ivorra & Morales, 1987) and after infection of DRG cells by herpes simplex virus (Mayer, 1986). I_H serves to shorten the duration of any after-hyperpolarization, being activated by hyperpolarization to potentials negative to about -70 mV, and tending to depolarize the membrane back towards potentials at which it is inactive. Impaired activity of the current thus increases the duration of after-hyperpolarizations. Curiously, the macroscopic current is very similar to a current expressed by the guard cells of plant leaf stomata which has been shown to be inactivated by a rise in $[Ca^{2+}]$ (Schroeder & Hagiwara, 1989), suggesting a striking conservation of channel properties (if it is indeed a similar channel).

The CN^--induced g_K may be used as an indirect indicator of $[Ca^{2+}]$. The conductance was increased despite the addition of ATP or an ATP-regenerating system to the cell via the patch pipette, suggesting that the rise in $[Ca^{2+}]$ proceeds independently of the $ATP/ADP.P_i$ ratio. The efficacy of added ATP in preventing wash-out of the Ca^{2+} current suggests that ATP does exchange adequately with the cytoplasm. These observations could be explained if the increased $[Ca^{2+}]$ is a consequence not of $[ATP]_i$ depletion, but rather of the fall in mitochondrial membrane potential, an expected response to all the agents used (see, for example, Kauppinen & Nicholls, 1986). Calcium is continuously cycled by mitochondria (Carafoli, 1979; Crompton, 1985; see Carafoli, 1987, for review), and, as influx is controlled by the mitochondrial membrane potential (Rottenberg & Scarpa, 1974), mitochondrial depolarization should reduce Ca^{2+} influx, accounting both for increased cytoplasmic $[Ca^{2+}]$ (see Heinonen *et al.* 1984) and impaired mitochondrial Ca^{2+} buffering (see Discussion in Duchen *et al.* 1990).

The initial response to impaired cell metabolism in the CNS appears to be neuronal hyperpolarization, decreasing excitability. The increased g_K documented in the present study would reduce the efficacy of synaptic input, shunting EPSPs. Similar effects have been described in hippocampal neurones by Fugiwara *et al.* (1987). This

may be functionally relevant in reducing depolarization-induced Ca^{2+} loading of the cells (see Duchen *et al.* 1990), as excessive and prolonged elevation of $[Ca^{2+}]$ may initiate irreversible cell injury (see Schanne, Kane, Young & Faber, 1979; Siesjö, 1981; Deshpande, Siesjö & Wieloch, 1987; Somjen, 1989). If presynaptic terminals express similar conductances, shunting of the membrane may block conduction of action potentials prevent transmitter release. The attenuation of the Ca^{2+} current may also reduce stimulus-coupled transmitter release from presynaptic terminals (Bosley, Woodhams, Gordon & Balasz, 1983; Adams *et al.* 1985). Elevated $[Ca^{2+}]_i$ may increase background, spontaneous transmitter release (Alnaes & Rahamimoff, 1975; Benveniste, Drejer, Schousboe & Diemer, 1984), decreasing the signal-to-noise ratio in the CNS. The combination of neuronal hyperpolarization, impaired synaptic transmission and such disruption of signal processing may well underlie the impairment of consciousness resulting from hypoxia or hypoglycaemia. Further release of excitatory amino acids may subsequently lead to depolarization and thence to excitotoxic neuronal injury (e.g. Van Harreveld, 1959; Clark & Rothman, 1987; for review, see Mayer & Westbrook, 1987).

REFERENCES

ADAMS, D. J., TAKEDA, K. & UMBACH, J. A. (1985). Inhibitors of calcium buffering depress evoked transmitter release at the squid giant synapse. *Journal of Physiology* **369**, 145–159.

ALNAES, E. & RAHAMIMOFF, R. (1975). On the role of mitochondria in transmitter release from motor nerve terminals. *Journal of Physiology* **248**, 285–306.

BACHELARD, H. S., COX, D. W. G., FEENEY, J. & MORRIS, P. G. (1985). ^{31}P nuclear magnetic resonance studies on superfused cerebral tissue. *Biochemical Society Transactions* **13**, 835–839.

BENVENISTE, H., DREJER, J., SCHOUSBOE, A. & DIEMER, N. H. (1984). Elevation of the extracellular concentrations of glutamate and aspartate in rat hippocampus during transient cerebral ischemia monitored by intracerebral microdialysis. *Journal of Neurochemistry* **43**, 1369–1374.

BERNARDI, H., FOSSET, M. & LAZDUNSKI, M. (1988). Characterization, purification and affinity labelling of the brain $[H^3]$-glibenclamide binding protein, a putative neuronal ATP-regulated K^+ channel. *Proceedings of the National Academy of Sciences of the USA* **85**, 9816–9820.

BISCOE, T. J. & DUCHEN, M. R. (1986). Synaptic physiology of spinal motoneurones of normal and *spastic* mice: an *in vitro* study. *Journal of Physiology* **379**, 275–292.

BISCOE, T. J. & DUCHEN, M. R. (1989). Electrophysiological responses of dissociated type I cells of the rabbit carotid body to cyanide. *Journal of Physiology* **413**, 447–468.

BISCOE, T. J., DUCHEN, M. R., EISNER, D. A., O'NEILL, S. C. & VALDEOLMILLOS, M. (1988). The effects of glucose removal and cyanide on intracellular calcium in isolated single mouse dorsal root ganglion cells. *Journal of Physiology* **401**, 60P.

BISCOE, T. J., DUCHEN, M. R., EISNER, D. A., O'NEILL, S. C. & VALDEOLMILLOS, M. (1989). Measurements of intracellular Ca^{2+} in dissociated type I cells of the rabbit carotid body. *Journal of Physiology* **416**, 421–434.

BLATZ, A. L. & MAGLEBY, K. L. (1987). Calcium-activated K^+ channels. *Trends in Neurosciences* **10**, 463–467.

BOSLEY, T. M., WOODHAMS, P. L., GORDON, R. D. & BALASZ, R. (1983). Effects of anoxia on the stimulated release of amino-acid neurotransmitters in the cerebellum in vitro. *Journal of Neurochemistry* **40**, 189–201.

BRANSTON, N. M., STRONG, A. J. & SYMON, L. (1977). Extracellular potassium activity, evoked potential and tissue flow. *Journal of Neurological Science* **32**, 305–321.

CARAFOLI, E. (1979). The calcium cycle of mitochondria. *FEBS Letters* **104**, 1–5.

CARAFOLI, E. (1987). Intracellular calcium homeostasis. *Annual Review of Biochemistry* **56**, 395–435.

CASTLE, N. A. & HAYLETT, D. G. (1987). Effect of channel blockers on potassium efflux from metabolically exhausted frog skeletal muscle. *Journal of Physiology* **383**, 31–43.

CHAD, J. E. & ECKERT, R. (1986). An enzymatic mechanism for calcium current inactivation in dialysed *Helix* neurones. *Journal of Physiology* **378**, 31–52.

CLARK, G. D. & ROTHMAN, S. M. (1987). Blockade of excitatory amino-acid receptors protects anoxic hippocampal slices. *Neuroscience* **21**, 665–671.

COOK, D. L. & HALES, N. (1984). Intracellular ATP directly blocks K^+ channels in pancreatic β-cells. *Nature* **311**, 271–274.

COX, D. W. G. & BACHELARD, H. S. (1982). Attenuation of evoked field potentials from dentate granule cells by low glucose, pyruvate + malate, and sodium fluoride. *Brain Research* **239**, 527–534.

COX, D. W. G., MORRIS, P. G., FEENEY, J. & BACHELARD, H. S. (1983). ^{31}P-n.m.r. studies on cerebral energy metabolism under conditions of hypoglycaemia and hypoxia *in vitro*. *Biochemical Journal* **212**, 365–370.

CROMPTON, M. (1985). The regulation of mitochondrial calcium transport in heart. *Current Topics in Membrane Transport* **25**, 231–276.

DESHPANDE, J. K., SIESJÖ, B. K. & WIELOCH, T. (1987). Calcium accumulation and neuronal damage in the rat hippocampus following cerebral ischemia. *Journal of Cerebral Blood Flow and Metabolism* **7**, 89–95.

DUCHEN, M. R. (1989). GABA$_A$ responses of dissociated mouse neurones are attenuated by metabolic blockade. *Journal of Physiology* **415**, 48P.

DUCHEN, M. R., CADDY, K. W. T., KIRBY, G. C., PATTERSON, D. L., PONTE, J. & BISCOE, T. J. (1988). Biophysical studies of the cellular elements of the rabbit carotid body. *Neuroscience* **26**, 291–313.

DUCHEN, M. R. & PEARCE, R. J. (1989). A preparation of neurones freshly dissociated from mouse dorsal root ganglia for electrophysiological study. *Journal of Physiology* **415**, 6P.

DUCHEN, M. R. & SOMJEN, G. G. (1988). Effects of cyanide and low glucose on the membrane currents of dissociated mouse primary sensory neurones. *Journal of Physiology* **401**, 61P.

DUCHEN, M. R., VALDEOLMILLOS, M., O'NEILL, S. C. & EISNER, D. A. (1990). On the regulation of intracellular calcium in isolated mouse sensory neurones. *Journal of Physiology* **424**, 411–427.

ECCLES, R. M., LOYNING, Y. & OSHIMA, T. (1966). Effects of hypoxia on the monosynaptic reflex pathway in the cat spinal cord. *Journal of Neurophysiology* **29**, 315–322.

FUJIWARA, N., HIGASHI, H., SHIMOJI, K. & YOSHIMURA, M. (1987). Effects of hypoxia on rat hippocampal neurones *in vitro*. *Journal of Physiology* **384**, 131–151.

GALLEGO, R., IVORRA, I. & MORALES, A. (1987). Effects of central or peripheral axotomy on membrane properties of sensory neurones in the petrosal ganglion of the cat. *Journal of Physiology* **391**, 39–56.

GLÖTZNER, F. (1967). Intracellular Potentiale, EEG und corticale Gleichspannung and der sensorimotorischen Rinde der Katze bei akuter Hypoxie. *Archiven der Psychiatrie und Nervenkranken* **210**, 274–296.

GODFRAIND, J. M., KAWAMURA, H., KRNJEVIĆ, K. & PUMAIN, R. (1971). Actions of dinitrophenol and some other metabolic inhibitors on cortical neurones. *Journal of Physiology* **215**, 199–222.

GROSSMAN, R. G. & WILLIAMS, V. F. (1971). Electrical activity and ultrastructure of cortical neurons and synapses in ischemia. *Clinics in Developmental Medicine* **39–40**, 61–75.

HAMILL, O. P., MARTY, A., NEHER, E., SAKMANN, B. & SIGWORTH, F. J. (1981). Improved patch-clamp technique for high-resolution current recording from cells and cell-free membrane patches. *Pflügers Archiv* **391**, 85–100.

HANSEN, A. J. (1985). Effects of anoxia on ion distribution in the brain. *Physiological Reviews* **65**, 101–148.

HANSEN, A. J., HOUNSGAARD, J. & JAHNSEN, H. (1982). Anoxia increases potassium conductance in hippocampal nerve cells. *Acta physiologica scandinavica* **115**, 301–310.

HARPER, A. A. & LAWSON, S. N. (1985). Electrical properties of rat dorsal root ganglion neurones with different peripheral nerve conduction velocities. *Journal of Physiology* **359**, 47–64.

HEINONEN, E., ÅKERMAN, K. E. O. & KAILA, K. (1984). Depolarization of the mitochondrial membrane potential increases free cytosolic calcium in synaptosomes. *Neuroscience Letters* **49**, 33–37.

KAUPPINEN, R. A. & NICHOLLS, D. G. (1986). Synaptosomal bioenergetics: the role of glycolysis, pyruvate oxidation and responses to hypoglycaemia. *European Journal of Biochemistry* **158**, 159–165.

KOSTYUK, P. G. (1984). Metabolic control of ionic channels in the neuronal membrane. *Neuroscience* **13**, 983–989.

KRNJEVIĆ, K. (1975). Coupling of neuronal metabolism and electrical activity. In *Brain Work (Alfred Benzon Symposium)*, ed. INGVAR, D. H. & LASSEN, N. A., pp. 65–78. Mundsgaard, Copenhagen.

KRNJEVIĆ, K. & LEBLOND, J. (1987). Mechanism of hyperpolarizing response of hippocampal calls to anoxia in isolated slices of rat hippocampus. *Journal of Physiology* **382**, 79P.

LATORRE, R., OBERHAUSER, A., LABARCA, P. & ALVAREZ, O. (1989). Varieties of calcium-activated potassium channels. *Annual Reviews of Physiology* **51**, 385–400.

LEE, K. S., MARBAN, E. & TSIEN, R. W. (1985). Inactivation of calcium channels in mammalian heart cells: joint dependence on membrane potential and intracellular calcium. *Journal of Physiology* **364**, 395–411.

LIPTON, P. & WHITTINGHAM, T. S. (1979). The effect of hypoxia on evoked potentials in the *in vitro* hippocampus. *Journal of Physiology* **287**, 427–438.

LIPTON, P. & WHITTINGHAM, T. S. (1982). Reduced ATP concentration as a basis for synaptic transmission failure during hypoxia in the *in vitro* guinea-pig hippocampus. *Journal of Physiology* **325**, 51–65.

LIU, C. & HERMANN, T. E. (1978). Characterization of ionomycin as a calcium ionophore. *Journal of Biological Chemistry* **253**, 5892–5894.

MAYER, M. L. (1985). A calcium-activated chloride current generates the after-depolarization of rat sensory neurones in culture. *Journal of Physiology* **364**, 217–240.

MAYER, M. L. (1986). Selective block of inward but not outward rectification in rat sensory neurones infected with herpes simplex virus. *Journal of Physiology* **375**, 327–338.

MAYER, M. L. & WESTBROOK, G. L. (1983). A voltage-clamp analysis of inward (anomalous) rectification in mouse spinal sensory ganglion neurones. *Journal of Physiology* **340**, 19–46.

MAYER, M. L. & WESTBROOK, G. L. (1987). Cellular mechanisms underlying excitotoxicity. *Trends in Neurosciences* **10**, 59–61.

MORAD, M., DAVIES, N. W., KAPLAN, J. K. & LUX, H. D. (1988). Inactivation and block of calcium channels by photoreleased Ca in dorsal root ganglion neurones. *Science* **241**, 842–844.

NACHSHEN, D. A. (1985). Regulation of cytosolic calcium concentration in presynaptic nerve endings isolated from rat brain. *Journal of Physiology* **363**, 87–101.

NICHOLLS, D. G. & ÅKERMAN, K. E. O. (1981). Biochemical approaches to the study of cytosolic calcium regulation in nerve endings. *Philosophical Transactions of the Royal Society* B **296**, 115–122.

NOMA, A. (1983). ATP-regulated K channels in cardiac muscle. *Nature* **305**, 147–148.

NOWYCKY, M. C., FOX, A. P. & TSIEN, R. W. (1985). Three types of neuronal calcium channel with different calcium agonist sensitivity. *Nature* **316**, 440–443.

OWEN, D. G., SEGAL, M. & BARKER, J. L. (1984). A Ca-activated Cl⁻ conductance in mouse cultured spinal neurons. *Nature* **311**, 567–570.

RASGADO-FLORES, H. & BLAUSTEIN, M. P. (1987). ATP-dependent regulation of cytoplasmic free calcium in nerve terminals. *American Journal of Physiology* **252**, C588–594.

ROTTENBERG, H. & SCARPA, A. (1974). Calcium uptake and membrane potential in mitochondria. *Biochemistry* **13**, 4811–4819.

SCHANNE, F. A. X., KANE, A. B., YOUNG, E. E. & FABER, J. L. (1979). Calcium-dependence of toxic cell death: a final common pathway. *Science* **206**, 700–702.

SCHROEDER, J. I. & HAGIWARA, S. (1989). Cytosolic calcium regulates ion channels in the plasma membrane of *Vicia faba* guard cells. *Nature* **338**, 427–430.

SIESJÖ, B. K. (1981). Cell damage in the brain: a speculative synthesis. *Journal of Cerebral Blood Flow and Metabolism* **1**, 155–185.

SOMJEN, G. G. (1989). Basic mechanisms in cerebral hypoxia and stroke. In *Mechanisms of Cerebral Hypoxia and Stroke, Advances in Behavioural Biology Series*, vol. 35, ed. SOMJEN, G. G. Plenum Press, New York.

VAN HARREVELD, A. (1959). Compounds in brain extracts causing spreading depression of cerebral cortical activity and contraction of crustacean muscle. *Journal of Neurochemistry* **3**, 300–315.